PHYSICAL REVIEW E **78**, 065701(R) (2008)

Biased random walks on a lattice: Exact numerical method to study the effect of alternating fields in disordered and asymmetric systems of obstacles

Francis A. Torres, Michel G. Gauthier, and Gary W. Slater
Department of Physics, University of Ottawa, 150 Louis-Pasteur, Ottawa, Ontario K1N 6N5, Canada
(Received 1 February 2008; revised manuscript received 30 October 2008; published 1 December 2008)

The migration of a particle in a system of obstacles under the action of an external field is often modeled using lattice Monte Carlo algorithms. For example, such simulation methods have been used to study the electrophoresis of charged molecules in sieving gels and the separation of particles using ratchet systems. In the case of constant fields or low-frequency alternating fields, the Monte Carlo simulation method can be mapped onto a numerical or algebraic matrix problem that can be solved exactly. In this Rapid Communication, we generalize this matrix approach to treat periodic time-dependent fields. The evolution of the spatial distribution function during a period is computed using a sequence of transfer matrices, and a steady-state closure relation allows us to calculate the exact mean velocity of the particle during a complete cycle. As an example, we examine the properties of a simple spatially asymmetric ratchet system in the presence of periodic alternating fields (symmetric and asymmetric) as well as random telegraph signals.

DOI: 10.1103/PhysRevE.78.065701 PACS number(s): 05.10.−a, 05.40.Jc, 82.20.Wt

Lattice Monte Carlo (LMC) simulation methods are very efficient and can be used to study a wide variety of diffusion-related problems [1–3]. Typically, a particle moves randomly between lattice sites in the presence of constraints (e.g., obstacles represented as forbidden lattice sites) and external fields. The connection between the real problem (continuous space, particle charge and friction coefficient, liquid viscosity, medium properties, etc.) and the discretized LMC representation is often subtle, and one must be careful in order to obtain the proper dynamics, especially at high field intensity [4].

Recently, we derived LMC algorithms that produce the right velocity and diffusion coefficient for arbitrary field intensities [4–7]. Some of these algorithms use a fixed time step, even though the jumps along and perpendicular to the field direction should in principle take different times if a field is present. With a fixed time step, it is possible to transform a stochastic LMC simulation into a matrix equation that can be solved exactly to obtain the steady-state velocity in the presence of obstacles. However, this numerical approach is limited to constant field intensities; standard computer simulations are required if the field intensities vary as a function of time.

Gel electrophoresis separations sometimes make use of pulsed electric fields to free particles from dead ends [8]. Although this method has been studied experimentally, very few theoretical or computational investigations have been published. Asymmetric dead-end traps can be used to improve separation using a mechanism called a ratchet [9–11]. Let us take, for example, the asymmetric system of obstacles shown in Fig. 1(a). In the presence of a symmetric alternating field, a unit size particle (size $a\times a$, as shown) will get trapped when the field is pointing in the $+\hat{x}$ direction, but not when it is reversed. Therefore, even if the external field has a mean value of zero during a cycle, the particle will show a net displacement in the negative direction. For this system, the trapping process is reversed for a $2a\times 2a$ particle. This is also a process that can be studied using LMC simulations, but exact solutions of the LMC algorithm can only be obtained in the limit where the pulse duration is infinite. Clearly, finite frequencies are of great interest because of the possibility of system optimization, current reversals (negative mobilities), and resonances [12].

In this Rapid Communication, we demonstrate that our matrix method can be generalized to treat finite frequencies. In brief, we use transfer matrices to transform the distribution function from one time step to the next, and we use the fact that the field is periodic to obtain a closure relation that applies to the steady state. Exact numerical results can thus be obtained, and subtle effects, essentially impossible to quantify using stochastic simulation methods, can be exam-

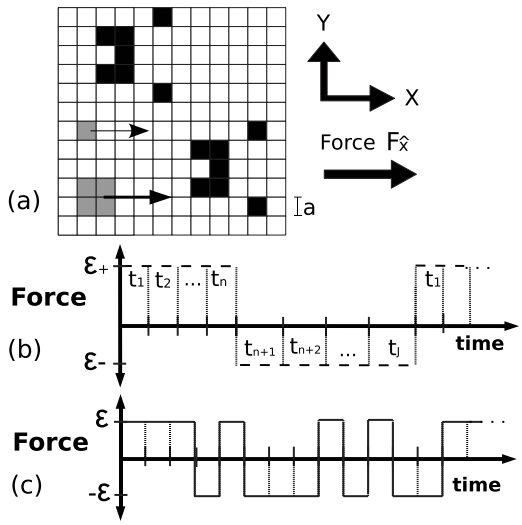

FIG. 1. (a) A 2D lattice with obstacles (black) and periodic boundary conditions. Particles of sizes $a\times a$ and $2a\times 2a$ (gray) jump to neighboring sites (if they are not occupied by obstacles) at every time step. Traps are asymmetric along the axis of the applied force. (b) A simple square pulse sequence. The total period of the sequence includes J Monte Carlo time steps. (c) In a random telegraph signal, the magnitude of the force is constant but the direction switches randomly.

ined. As an example, we study the two-dimensional (2D) ratchet system shown in Fig. 1(a).

A particle of radius R moves in a liquid of viscosity η under the action of an external force $\vec{F}=+F\hat{x}$. The particle's friction coefficient is then given by $\xi(R)=6\pi\eta R$, and its diffusion coefficient is $D_0(R)=k_BT/\xi(R)$. Its velocity is given by the relation $v_0=F/\xi$. The corresponding LMC model uses a lattice with a mesh size a [Fig. 1(a)] and periodic boundary conditions. The particle then makes jumps of size a in one of the four directions at each time step. In the absence of a force, the basic time step is $\tau_B(R)=a^2/2D_0(R)$. In terms of the Brownian time $\tau_B(R)\sim R$ and the lattice mesh size a, we can write

$$v_0=\frac{F}{\xi}=\frac{FD_0}{k_BT}=\varepsilon\frac{a}{\tau_B}, \tag{1}$$

where $\varepsilon=Fa/2k_BT$ is the dimensionless force [5].

We now consider the 2D system in Fig. 1(a). In the presence of a constant force of magnitude ε, it is possible to use the following time step for both x and y jumps:

$$\tau(\varepsilon)=\frac{\tau_B}{1+\varepsilon\coth(\varepsilon)}, \tag{2}$$

where $\tau(0)=\tau_B/2$, as expected. The transition probabilities are then given by

$$P_{\pm x}(\varepsilon)=\frac{1}{(1+e^{\mp 2\varepsilon})[1+\tanh(\varepsilon)/\varepsilon]}, \tag{3}$$

$$P_{\pm y}(\varepsilon)=\frac{\tau(\varepsilon)}{2\tau_B}. \tag{4}$$

We note that $P_{\pm x}=P_{\pm y}=1/4$ when $\varepsilon=0$, as expected for an unbiased process. It is easy to show that these LMC parameters recover the free-solution velocity and diffusion coefficient (v_0 and D_0) for arbitrary magnitudes of the force if there is no obstacle in the system. As usual, Monte Carlo steps that lead to the particle overlapping with an obstacle are rejected. The particle properties can impact the results via the scaled force ε (e.g., for a fixed external field, the resulting force may depend on the particle's charge or mass), and the size R (which affects both the number of collisions with the obstacles and the Brownian time τ_B). The field lines are considered straight and unaffected by the obstacles.

Although it is easy to use this LMC algorithm to simulate systems with obstacles and constant external forces, one can solve the algorithm exactly using the following method, which we described in detail in previous publications [5,13]. Let $|n(t)\rangle$ be the state vector containing the particle's probabilities of presence $n_i(t)$ on each of the lattice sites i at time step t (we use the bra-ket Dirac notation to represent row and column vectors). Given the probabilities $P_{\pm y}$ and $P_{\pm x}$ and the location of the obstacles on the lattice, one can write a transfer matrix A such that the distribution function after the next Monte Carlo jump is given by the matrix operation

$$|n[t+\tau(\varepsilon)]\rangle=A|n(t)\rangle. \tag{5}$$

Of course, this can be done only if we have the same time duration for all jumps. If the force ε is constant, the matrix $A=A(\varepsilon)$ is itself time independent. Equation (5) can then be used iteratively to calculate all future distribution functions $|n(t)\rangle$ given an initial distribution $|n(0)\rangle$. However, since we are looking for the mean particle velocity for long times, one can use the simple relation $|n(t)\rangle=|n(t+\tau(\varepsilon))\rangle\equiv|n\rangle$ to compute the distribution function $|n\rangle$ in the steady state. This matrix equation, together with the normalization condition $\langle 1|n\rangle=1$, can be solved numerically with arbitrary precision, or even algebraically in some cases. For a given obstacle configuration, the mean velocity of the particle when it is located on lattice site i is given by

$$\overline{v}_i=\frac{a(P_{+x}L_{+i}-P_{-x}L_{-i})}{\tau(\varepsilon)}, \tag{6}$$

where $L_{\pm i}=0$ if the target site is occupied by an obstacle and $L_{\pm i}=1$ if it is free. With the row vector $\langle v|$ containing the local mean velocities thus calculated, the mean global velocity in the steady state is simply given by the weighted average $\overline{V}_x=\langle v|n\rangle$. Figure 2(a) shows the result of this calculation for the system shown in Fig. 1(a) for constant forces $-1\leqslant\varepsilon\leqslant 4$ and two particles with different sizes (the force applied to the two particles is the same). In both cases, the particle eventually has a negligible velocity because it gets trapped inside the dead ends. The maxima are found at $\varepsilon_1\approx 1.02$ and $\varepsilon_2\approx -0.38$ for the small and large particle, respectively (note the different signs).

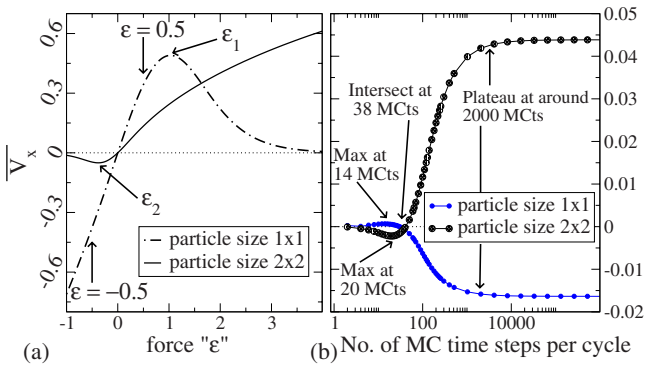

FIG. 2. (Color online) (a) Net velocity vs the amplitude of the external dc force (pointing in the $+\hat{x}$ direction) for the system shown in Fig. 1(a). The maxima are located at $\varepsilon_1\approx 1.02$ and $\varepsilon_2\approx -0.38$. (b) Net velocity vs the duration of the square-pulse ac cycle (with $\varepsilon=\pm 0.5$) for the system shown in Fig. 1(a). The lines cross at cycle durations of about 38 MC time steps (MCts). The plateaus are at −0.0163 and 0.0439.

Our goal here is to extend the usefulness of our exact numerical method to time-varying but periodic external forces. Figure 1(b) gives an example where only two scaled forces are used, ε_+ and ε_-. A general force cycle is a sequence of J potentially different LMC conditions where the force is ε_j at time t_j, with $j=1,\ldots,J$. Note that the duration of the LMC steps changes for each instantaneous value of ε_j so that $t_{j+1}-t_j=\tau(\varepsilon_j)$. Because time is discretized, a LMC method is not expected to be reliable at very high frequency (i.e., if $J\approx 1$).

The evolution of the distribution function can now be calculated iteratively using matrix relations such as

$$A_1|n(t_1)\rangle = |n(t_2)\rangle, \tag{7}$$

$$A_2|n(t_2)\rangle = |n(t_3)\rangle, \tag{8}$$

$$\vdots$$

$$A_{J-1}|n(t_{J-1})\rangle = |n(t_J)\rangle. \tag{9}$$

We use this numerical method only for systems that do not have separate unconnected zones. In such cases, the transition matrices A_i are not block diagonal, and multiplying them to generate the future states of the system eventually yields regular stochastic matrices, i.e., transition matrices where all entries are greater than 0 [14]; the latter are known to produce Markov chains that possess a steady state [14]. Therefore, we can close the sequence of operations described by Eqs. (7)–(9) using the relation

$$\left(\prod_{j=1}^{J}(A_{J-j+1})\right)|n(t_1)\rangle = |n(t_1)\rangle. \tag{10}$$

This essentially defines a transfer matrix $A_{J1} \equiv A_J \times A_{J-1} \times \cdots \times A_1$ which allows us to compute the steady-state beginning-of-the-cycle distribution function $|n(t_1)\rangle$. Once this is computed, the A_j matrices can be used to iteratively compute the steady-state distribution functions $|n(t_j)\rangle$ for the rest of the cycle (i.e., for $j=2,\ldots,J$). We note, however, that the time duration of the various LMC steps j may differ from each other. The total period of the cycle is thus given by $\Sigma_1^J \tau(\varepsilon_j)$. For each LMC jump j, one can also write a row vector $\langle v(t_j)|$ containing the instantaneous mean velocities $v_i(t_j)$ on each site i. The mean distance migrated during a given LMC time step is thus given by $\Delta x(t_j) = \tau(\varepsilon_j)\langle v(t_j)|n(t_j)\rangle$. Finally, the mean velocity during a complete steady-state cycle is

$$\overline{V_x} = \frac{\sum_{j=1}^{J}\Delta x(t_j)}{\sum_{j=1}^{J}\tau(\varepsilon_j)} = \frac{\sum_{j=1}^{J}\langle v(t_j)|n(t_j)\rangle \times \tau(\varepsilon_j)}{\sum_{j=1}^{J}\tau(\varepsilon_j)}. \tag{11}$$

This completes the procedure to follow to obtain exact numerical results for LMC problems that include periodic time-varying forces.

In order to demonstrate the usefulness of our numerical method, we examine the behavior of the two particles migrating in the system shown in Fig. 1(a) when we apply symmetric and asymmetric pulsed fields. We also investigate the response of this system to random telegraph signals. The dc data were shown in Fig. 2(a).

First, we apply a symmetric ac force [Fig. 1(b), with $J=2n$ and $\varepsilon_+ = -\varepsilon_-$]. We are computing the net velocity as a function of the number of Monte Carlo time steps (MCts) per cycle; the results are shown in Fig. 2(b). The geometric asymmetry of the system of obstacles leads to nonzero net velocities in spite of the fact that the mean force (over a complete ac cycle) is zero. We note that the particles almost always move in opposite directions, and that their net velocities are equal when the cycle duration is about 38 MCts [see Fig. 2(b)]. These velocities then increase with increasing cycle duration up to a plateau limit starting at about 2000 MCts. For very long cycle durations, the plateau result is simply the average of the two dc velocities; the latter can be obtained from Fig. 2(a) (they are marked by the two arrows). It is clear from Fig. 2(b) that application of an unbiased ac force could be a useful way to exploit the geometric asymmetry to build a powerful sieving system where particles of different sizes move in opposite directions [11,12].

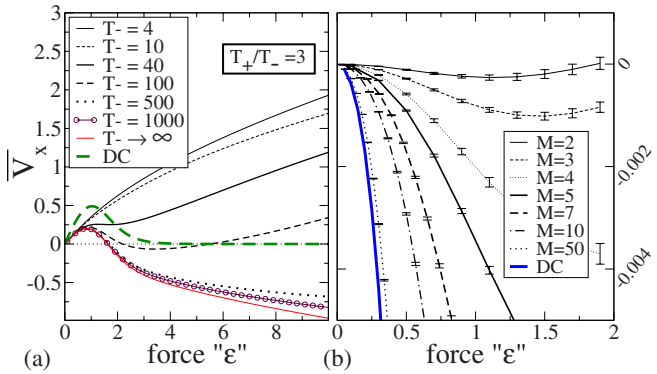

FIG. 3. (Color online) (a) Net velocity vs the amplitude of the external ac force for the small particle in the system shown in Fig. 1(a). The square-pulse asymmetric ac force is $+\varepsilon$ for a duration T_+, and $-\varepsilon$ for a duration T_-. The ratio T_+/T_- is kept fixed at 3. The long-dashed curve shows the velocity in the presence of a dc force [see Fig. 2(a)]. (b) Here, the ac force is a random telegraph signal which alternates randomly between $\pm\varepsilon$ [the mean force is thus zero; see Fig. 1(c)]. We varied the number M of consecutive MC steps with the same force value.

Field inversion gel electrophoresis (FIGE) [15] generally uses biased pulsed electric fields where the field direction is reversed periodically (the amplitude is kept constant) and the forward pulse duration T_+ is longer than the reverse pulse duration T_- (a ratio $T_+/T_- \cong 3$ is typical). We now examine the effect of such FIGE conditions for the small particle in the system shown in Fig. 1(a). Of course, reversing the field direction periodically will help the particle move out of the steric traps (in dc fields, only thermally activated escapes are allowed) [8]. The results are shown in Fig. 3(a); note that the long-dashed curve shows the data for a dc field [these are the data found in Fig. 1(a)]. As expected, the average of three positive dc fields with one negative dc field (bottom curve, marked $T_- \to \infty$) is recovered for very long pulses. At high frequency, the net velocity increases with field intensity as if we had a dc force of amplitude $[(T_+ - T_-)/(T_+ + T_-)]\varepsilon = \frac{1}{2}\varepsilon$ and no trapping (compare the dc line and the $T_-=4$, 10, or 40 line). The high-frequency and dc curves cross at $\epsilon \approx 1.36$; beyond this point, the velocity is higher with the high-frequency ac force (because of the detrapping effects) even though the particle moves backward 25% of the time. At $T_- \simeq 40$, the net ac velocity plateaus between $\varepsilon \simeq 1$ and $\varepsilon \simeq 2$, but keeps increasing afterward. For longer pulses, the velocity reaches a maximum at $\varepsilon \simeq 1$ and decreases for higher fields before it increases again. As the $T_-=100$ case

shows, one can even see two velocity reversals as the force is increased (this small double reversal would be almost impossible to observe using LMC simulations). For very long pulses, we observe only one velocity reversal and the net mobility is negative for all forces beyond about $\varepsilon \simeq 1.64$. We note that, for a fixed value of ε, a reversal of the net velocity is also observed when changing the pulse duration if the force is large enough.

Finally, we apply a random telegraph signal to the same system. The signal is made of pulses of duration $M\tau(\varepsilon)$ and random intensities $\pm\varepsilon$ [see Fig. 1(c)]. For our algorithm to work, we must have the same number of positive and negative pulses (i.e., an unbiased random force), and the sequence must be periodic. We thus use very long cycles [typically of duration $10^5\tau(\varepsilon)$] that mimic nonperiodic conditions (the round-up error introduced by the large number of matrix multiplications was less than 10^{-5} in all cases), and we average over a large number of random permutations of the $\pm$ pulses. Here, M acts like a correlation time for the random telegraph signal. As M gets very long, we recover the dc limit of two dc forces averaged together. Again, we observe nonzero velocities in the presence of an ac force with a zero mean value. However, the velocities are always negative here [unlike the case of Fig. 2(b)], showing that random telegraph signals are fundamentally different from strictly periodic ac signals. At high frequency, the velocity is essentially zero, while it was slightly positive in Fig. 2(b). Moreover, we note a rapid change as the correlation time increases from $M=2$ to 5. This is due to the fact that, at high force strength, it takes about five jumps to move from one row of obstacles to the next in Fig. 1(a).

In conclusion, we presented a generalized matrix method that can be used to compute the exact numerical solution for lattice Monte Carlo simulations in the presence of time-varying but periodic forces. The method is simple to use but it requires important memory resources if the lattice is large. We showed the power of this method by investigating a simple toy model with asymmetric obstacles that lead to ratchet effects and current reversals. Some of the effects found here would be essentially impossible to observe using stochastic methods. Our method can easily treat a wide variety of periodic signals such as sinusoidal functions (made of histograms), pseudorandom pulses, or even fields that switch between the x and y directions.

G.W.S. gratefully acknowledges the support of the Natural Science and Engineering Research Council (NSERC) of Canada.

[1] M. E. J. Newman and G. T. Barkema, *Monte Carlo Methods in Statistical Physics* (Oxford University Press, Oxford, 1999).
[2] I. Majid, D. Ben-Avraham, S. Havlin, and H. E. Stanley, Phys. Rev. B **30**, 1626 (1984).
[3] P. Grassberger, G. T. Barkema, and W. Nadler, *Monte Carlo Approach to Biopolymers and Protein Folding* (World Scientific, Singapore, 1998).
[4] M. G. Gauthier and G. W. Slater, Phys. Rev. E **70**, 015103(R) (2004).
[5] M. G. Gauthier and G. W. Slater, J. Chem. Phys. **117**, 6745 (2002).
[6] J.-F. Mercier, F. Tessier, and G. W. Slater, Electrophoresis **22**, 2631 (2001).
[7] M. G. Gauthier and G. W. Slater, Electrophoresis **24**, 441 (2003).
[8] K. Y. To and T. R. C. Boyde, Electrophoresis **14**, 597 (1993).
[9] R. D. Astumian and P. Hanggi, Phys. Today **55** (11), 33 (2002).
[10] X. Z. Cheng, M. B. A. Jalil, and H. K. Lee, Phys. Rev. Lett. **99**, 070601 (2007).
[11] J. Regtmeier, R. Eichhorn, T. T. Duong, P. Reimann, D. Anselmetti, and A. Ros, Eur. Phys. J. E **22**, 335 (2007).
[12] C. Desruisseaux, G. W. Slater, and T. B. L. Kist, Biophys. J. **75**, 1228 (1998).
[13] J.-F. Mercier, G. W. Slater, and H. L. Guo, J. Chem. Phys. **110**, 6050 (1999).
[14] W. K. Nicholson, *Linear Algebra with Applications*, 3rd ed. (PWS, Boston, 1995), p. 102, Theorem 2.
[15] C. Heller and F. M. Pohl, Nucleic Acids Res. **18**, 6299 (1990).